2 janvier 2023

Rapport Bureau d'Etude
Méthode de Galërkin Discontinu

Paul CALOT, Giuliano VINCI

Introduction

Across the methods to numerically integrate coupled wave equations, Discontinuous Galërkin methods have an edge w.r.t. several other possible choices, in that they enable the mathematician to vary more freely the thickness of the meshing. In this BE, several problems are mathematically described and their numerical solution, obtained via the Discontinuous Galërkin method, is exposed.

Question 1

Q1.1: Proving the Discontinuous Galërkin representation is correct

Showing the substantial equivalency between the differential Maxwell Equations and its DG formulation relies on a certain common framework. The differential Maxwell Problem, indeed, must be formulated in such a way:

$$\begin{cases} \lambda(\mathbf{x})\frac{\partial \mathbf{u}(\mathbf{x},t)}{\partial t} + \mathcal{A}\mathbf{v}(\mathbf{x},t) = \mathbf{f}(\mathbf{x},t) \quad in\ \ \Omega \\ \kappa(\mathbf{x})\frac{\partial \mathbf{v}(\mathbf{x},t)}{\partial t} - \mathcal{A}^*\mathbf{u}(\mathbf{x},t) = 0 \quad in\ \ \Omega \\ \mathcal{A}^*(\mathbf{n})\mathbf{u} = 0 \quad on\ \Gamma \\ \mathbf{u}(\mathbf{x},0) = \mathbf{u}_0 \quad in\ \ \Omega \\ \mathbf{v}(\mathbf{x},0) = \mathbf{v}_0 \quad in\ \ \Omega \end{cases} \tag{1}$$

Taking into account the structure specified for the equations in the assignments, it is possible to link some quantities in a way to show that the problem can be formulated with Galërkin formalism. In particular we find, assuming that $\mathbf{u} = \mathbf{E}$ and $\mathbf{v} = H$:

$$\mathcal{A}(\cdot) = -\nabla \times (\cdot) \quad -\mathcal{A}^*(\cdot) = \nabla \times (\cdot) \tag{2}$$

$$\lambda(\mathbf{x}) = \varepsilon(\mathbf{x}) \quad \kappa(\mathbf{x}) = \mu(\mathbf{x}) \tag{3}$$

$$\mathcal{A}^*(\mathbf{n})\mathbf{u} \equiv \mathbf{n} \times \mathbf{u} = 0 \implies \mathbf{E} \times \mathbf{n} = 0 \quad on\ \Gamma \tag{4}$$

$$\mathbf{f}(\mathbf{x},t) = \mathbf{J}(\mathbf{x},t) \tag{5}$$

With the mentioned assumptions, one obtains easily:

$$\begin{cases} \varepsilon\frac{\partial \mathbf{E}}{\partial t} - \nabla \times H = \mathbf{J}(\mathbf{x},t) \quad in\ \ \Omega \\ \mu\frac{\partial H}{\partial t} + \nabla \times \mathbf{E} = 0 \quad in\ \ \Omega \\ \mathbf{E} \times \mathbf{n} = 0 \quad on\ \Gamma \\ \mathbf{E}(\mathbf{x},0) = \mathbf{E}_0 \quad in\ \ \Omega \\ H(\mathbf{x},0) = H_0 \quad in\ \ \Omega \end{cases} \tag{6}$$

One can notice easily that the boundary condition stands for a perfectly conductive medium, which has electric field to be normal to its surface. The procedure used to obtain the integral equations will be described shortly hereafter.

Bootstrapping the procedure:

Applying the general theory on discontinuous Galërkin methods (from now on "DG") for problems expressed as in 1, the two differential equations are multiplied by some proper test functions $\mathbf{v}_h$ and w_h, living in the proper spaces of Electric and Magnetic fields, respectively.

Result of the first IBP:

They are henceforth integrated on their domains. By applying an Integration By Parts (IBP), the following results are obtained:

$$\frac{d}{dt}\iiint_T \varepsilon \mathbf{E}_h \cdot \mathbf{v}_h \, d\mathbf{x} - \iiint_T H_h \cdot (\nabla \times \mathbf{v}_h) \; d\mathbf{x} + \oiint_{\partial T \setminus \Gamma} (\{\{H_h\}\} \times \mathbf{n}) \cdot \mathbf{v}_{h|T} \, d\gamma + \\ + \oiint_{\partial T \cap \Gamma} (H_h \times \mathbf{n}) \cdot \mathbf{v}_{h|T} \, d\gamma = \iiint_T \mathbf{J} \cdot \mathbf{v}_h \, d\mathbf{x}$$

$$\frac{d}{dt}\iiint_T \mu H_h w_h \, d\mathbf{x} + \iiint_T \mathbf{E}_h \cdot (\nabla \times w_h) \; d\mathbf{x} - \oiint_{\partial T \setminus \Gamma} (\{\{\mathbf{E}_h\}\} \times \mathbf{n}) \cdot w_{h|T} \, d\gamma = 0$$

where h is an index ranging on the subdomains of the mesh, and T is a cell of the meshing $\mathcal{T}_h$.

Reworking the equations with a second IBP:

The first equation is then reworked a second time with an IBP, leading to the following results as stated in the theory treating general $\mathcal{A}$ operators.

$$\frac{d}{dt}\iiint_T \varepsilon \mathbf{E}_h \cdot \mathbf{v}_h \, d\mathbf{x} - \iiint_T (\nabla \times H_h) \cdot \mathbf{v}_h \, d\mathbf{x} - \frac{1}{2}\oiint_{\partial T \setminus \Gamma} \big(\llbracket H_h \rrbracket \times \mathbf{n}\big) \cdot \mathbf{v}_{h|T} \, d\gamma = \iiint_T \mathbf{J} \cdot \mathbf{v}_h \, d\mathbf{x} \tag{7}$$

$$\frac{d}{dt}\iiint_T \mu H_h w_h \, d\mathbf{x} + \iiint_T \mathbf{E}_h \cdot (\nabla \times w_h) \; d\mathbf{x} - \oiint_{\partial T \setminus \Gamma} (\{\{\mathbf{E}_h\}\} \times \mathbf{n}) \cdot w_{h|T} \, d\gamma = 0 \tag{8}$$

We can now implement a couple of simple devices (such as changing the order of signs or exploiting the cyclic property of vector product):

$$\frac{d}{dt}\iiint_T \varepsilon \mathbf{E}_h \cdot \mathbf{v}_h \, d\mathbf{x} - \iiint_T (\nabla \times H_h) \cdot \mathbf{v}_h \, d\mathbf{x} + \frac{1}{2}\oiint_{\partial T \setminus \Gamma} \big(\mathbf{n} \times \llbracket H_h \rrbracket\big) \cdot \mathbf{v}_{h|T} \, d\gamma = \iiint_T \mathbf{J} \cdot \mathbf{v}_h \, d\mathbf{x} \tag{9}$$

$$\frac{d}{dt}\iiint_T \mu H_h w_h \, d\mathbf{x} + \iiint_T \mathbf{E}_h \cdot (\nabla \times w_h) \; d\mathbf{x} - \oiint_{\partial T \setminus \Gamma} \{\{\mathbf{E}_h\}\} \cdot \big(\mathbf{n} \times w_{h|T}\big) \; d\gamma = 0 \tag{10}$$

The only missing terms w.r.t. the ones mentioned in the Sujet are the dissipation terms, which are discussed in the next subsection:

Adding a dissipation term for better stability:

In order to improve continuity of the solution and to increase stability in the numerical method, some penalisation operators are added. Applying the general theory, it is understood that the terms needed look

as such:

$$p_E(\mathbf{E}, \mathbf{v}_h) = \alpha_E \oiint_{\partial T \setminus \Gamma} \left(\mathcal{A}^*(\mathbf{n}_h)[\![\mathbf{E}_h]\!]\right) \cdot \left(\mathcal{A}^*(\mathbf{n}_h)[\![\mathbf{v}_h]\!]\right) \, d\gamma = \tag{11}$$

$$= \alpha_E \oiint_{\partial T \setminus \Gamma} \left([\![\mathbf{E}_h]\!] \times \mathbf{n}_h\right) \cdot \left([\![\mathbf{v}_{h|T}]\!] \times \mathbf{n}_h\right) \, d\gamma = \tag{12}$$

$$= \alpha_E \oiint_{\partial T \setminus \Gamma} \left([\![\mathbf{n}_h \times \mathbf{E}_h]\!]\right) \cdot \left(\mathbf{n}_h \times \mathbf{v}_{h|T}\right) \, d\gamma \tag{13}$$

$$p_H(H, w_h) = \alpha_H \oiint_{\partial T \setminus \Gamma} \left(\mathcal{A}^*(\mathbf{n}_h)[\![H_h]\!]\right) \cdot \left(\mathcal{A}^*(\mathbf{n}_h)[\![w_h]\!]\right) \, d\gamma = \tag{14}$$

$$= \alpha_H \oiint_{\partial T \setminus \Gamma} \left([\![H_h]\!] \times \mathbf{n}_h\right) \cdot \left([\![w_{h|T}]\!] \times \mathbf{n}_h\right) \, d\gamma = \tag{15}$$

$$= \alpha_H \oiint_{\partial T \setminus \Gamma} \left([\![\mathbf{n}_h \times H_h]\!]\right) \cdot \left(\mathbf{n}_h \times w_{h|T}\right) \, d\gamma \tag{16}$$

$$\tag{17}$$

As follows from the properties of the involved fields. Apart from showing the requested equivalence, this also leads to the following operatorial representation of the problem:

$$\begin{cases} \frac{d}{dt}\mathfrak{m}_E(\mathbf{E}^h, \mathbf{v}^h) + \mathfrak{a}(H^h, \mathbf{v}^h) + \mathfrak{p}_E(\mathbf{E}^h, \mathbf{v}^h) = \mathfrak{l}(\mathbf{v}^h) \quad \forall \mathbf{v}_h \\ \frac{d}{dt}\mathfrak{m}_H(H^h, w^h) - \mathfrak{a}(w^h, \mathbf{E}^h) + \mathfrak{p}_H(H^h, w^h) = 0 \quad \forall w_h \end{cases} \tag{18}$$

Q1.2: Specifying the matrix characteristics

From the operatorial representation, a matrix representation can be deduced and the properties of the matrices discussed:

$$\begin{cases} M^E \frac{d\mathbf{E}}{dt} + R\mathbf{H}(t) + P_E\mathbf{E}(t) = \mathbf{F}(t) \\ M^H \frac{d\mathbf{H}}{dt} - R^T\mathbf{E}(t) + P_H\mathbf{H}(t) = 0 \\ \mathbf{E}(0) = \mathbf{E}_0 \\ \mathbf{H}(0) = \mathbf{H}_0 \end{cases} \tag{19}$$

As for the matrices:

- M^E and M^H are the mass matrices for electric and magnetic fields, respectively. They are block diagonal (which follows from the absence of continuity constraints on the shape functions) and, at least, positive semi-definite.
- R is a sparse stiffness matrix.
- P_E and P_H are sparse penalisation matrices.

Question 2

Q2.1: Assigning E^0 and $H^{1/2}$

As it is clear for a leap-frog scheme, the useful initial conditions on $\mathbf{E}$ and H are not meant in the same time instant. For this reason, $\mathbf{E}^0$ and $H^{\frac{1}{2}}$ need to be assigned.

- $\mathbf{E}^0 = \mathbf{E}(t = 0)$;
- $H^{\frac{1}{2}} = H(\frac{\Delta t}{2}) = H(0) + \frac{\Delta t}{2}\frac{dV}{dt}(0) + O((\Delta t)^2) = H^0 - \frac{\Delta t}{2}(M^H)^{-1}R^T\mathbf{E}_0$.

The latter equation is easily explained with a Taylor expansion, needed to ensure consistency with second order time-accuracy of the scheme. Losing one order of accuracy, one can approximate $H^{\frac{1}{2}} \approx H^0$.

Q2.2: Showing the conservation of energy

In the absence of penalisation and source terms, energy conservation is shown both in the continuous and in the discrete case. The starting point is the complete discretised scheme:

$$\begin{cases} M^E \frac{E^{n+1}-E^n}{\Delta t} - RH^{n+\frac{1}{2}} + P^E E^n = F^{n+\frac{1}{2}} \\ M^H \frac{H^{n+\frac{3}{2}}-H^{n+\frac{1}{2}}}{\Delta t} + R^T E^{n+1} + P^H H^{n-\frac{1}{2}} = 0 \end{cases}$$

From which we eliminate the term F, encoding external sources, and P^H, P^E, penalisation terms which produce a negative energy balance (thus stabilising the system, at a cost of an unphysical energy loss in the numerical integration).

$$\begin{cases} M^E \frac{E^{n+1}-E^n}{\Delta t} - RH^{n+\frac{1}{2}} = 0 \\ M^H \frac{H^{n+\frac{3}{2}}-H^{n+\frac{1}{2}}}{\Delta t} + R^T E^{n+1} = 0 \end{cases}$$

I: Testing the first equation

We start the procedure by testing the first equation by $\frac{E^{n+1}+E^n}{2}$, as follows:

$$\begin{aligned} \mathbf{I}: \quad \left[M^E\left(\frac{E^{n+1}-E^n}{\Delta t}\right) - RH^{n+\frac{1}{2}}\right] \cdot \left(\frac{E^{n+1}+E^n}{2}\right) = 0 \implies \\ \frac{1}{2}\left[\frac{\left(M^E E^{n+1}, E\right) - \left(M^E E^n, E^n\right)}{\Delta t}\right] - \left(R^T \frac{E^{n+1}+E^n}{2}, H^{n+\frac{1}{2}}\right) = 0 \implies \\ \frac{1}{2}\left[\frac{\left(M^E E^{n+1}, E^{n+1}\right) - \left(M^E E^n, E^n\right)}{\Delta t}\right] - \frac{1}{2}\left(R^T E^{n+1}, H^{n+\frac{1}{2}}\right) - \frac{1}{2}\left(R^T E^n, H^{n+\frac{1}{2}}\right) = 0 \end{aligned}$$

II: Testing the second equation

Now the second equation is tested by $\frac{H^{n+\frac{1}{2}}}{2}$, but at two different times: $t = n$ and $t = n + 1$

$$\textbf{IIa}: \quad \left(M^H \frac{H^{n+\frac{1}{2}} - H^{n-\frac{1}{2}}}{\Delta t} + R^T E^n, \frac{H^{n+\frac{1}{2}}}{2} \right) = 0 \implies$$

$$\frac{1}{2} \frac{\left(M^H H^{n+\frac{1}{2}}, H^{n+\frac{1}{2}} \right) - \left(M^H H^{n-\frac{1}{2}}, H^{n+\frac{1}{2}} \right)}{\Delta t} + \frac{1}{2} \left(R^T E^n, H^{n+\frac{1}{2}} \right) = 0$$

$$\textbf{IIb}: \quad \left(M^H \frac{H^{n+\frac{3}{2}} - H^{n+\frac{1}{2}}}{\Delta t} + R^T E^{n+1}, \frac{H^{n+\frac{1}{2}}}{2} \right) = 0 \implies$$

$$\frac{1}{2} \frac{\left(M^H H^{n+\frac{3}{2}}, H^{n+\frac{1}{2}} \right) - \left(M^H H^{n+\frac{1}{2}}, H^{n+\frac{1}{2}} \right)}{\Delta t} + \frac{1}{2} \left(R^T E^{n+1}, H^{n+\frac{1}{2}} \right) = 0$$

III: Conservation law

In order to obtain the sought after conservation law, the three equations are summed together as follows:

$$\textbf{I} + \textbf{IIa} + \textbf{IIb} = 0$$

The sum is resumed hereafter, indicating all the terms which cancel out:

$$\frac{1}{2} \left[\frac{\left(M^E E^{n+1}, E^{n+1} \right) - \left(M^E E^n, E^n \right)}{\Delta t} \right] - \cancel{\frac{1}{2} \left(R^T E^{n+1}, H^{n+\frac{1}{2}} \right)} - \cancel{\frac{1}{2} \left(R^T E^n, H^{n+\frac{1}{2}} \right)} +$$

$$\cancel{\frac{1}{2} \frac{\left(M^H H^{n+\frac{1}{2}}, H^{n+\frac{1}{2}} \right) - \left(M^H H^{n-\frac{1}{2}}, H^{n+\frac{1}{2}} \right)}{\Delta t}} + \cancel{\frac{1}{2} \left(R^T E^n, H^{n+\frac{1}{2}} \right)} +$$

$$\cancel{\frac{1}{2} \frac{\left(M^H H^{n+\frac{3}{2}}, H^{n+\frac{1}{2}} \right) - \left(M^H H^{n+\frac{1}{2}}, H^{n+\frac{1}{2}} \right)}{\Delta t}} + \cancel{\frac{1}{2} \left(R^T E^{n+1}, H^{n+\frac{1}{2}} \right)} =$$

$$0$$

Eventually, we end up with:

$$\frac{1}{2} \frac{\left(M^E E^{n+1}, E^{n+1} \right) + \left(M^H H^{n+\frac{3}{2}}, H^{n+\frac{1}{2}} \right)}{\Delta t} = \tag{20}$$

$$\frac{1}{2} \frac{\left(M^E E^n, E^n \right) + \left(M^H H^{n-\frac{1}{2}}, H^{n+\frac{1}{2}} \right)}{\Delta t} \tag{21}$$

Which turns out to be the requested conservation law. Indeed, if the discreet energy $\mathcal{E}_h^n$ is defined as follows:

$$\mathcal{E}_h^n := \frac{1}{2} \left[\left(M^E E^n, E^n \right) + \left(M^H H^{n-\frac{1}{2}}, H^{n+\frac{1}{2}} \right) \right]$$

Then what we proved amounts to what was meant to be shown:

$$\mathcal{E}_h^{n+1} = \mathcal{E}_h^n \; \forall n \implies \mathcal{E}_h^n = \mathcal{E}_h^0 \; \forall n$$

Q2.3: Showing the CFL condition

Regarding the previously exposed conservation law, it is clever to exploit it also to assure the L^2 stability of the DG Method. Let's start by defining some norms:

$$\|\mathbf{E}\|_{0,\varepsilon}^2 := \left(M^E\mathbf{E}, \mathbf{E}\right) \tag{22}$$

$$\|\mathbf{H}\|_{0,\mu}^2 := \left(M^H\mathbf{H}, \mathbf{H}\right) \tag{23}$$

$$\|\ (\mathbf{E}, \mathbf{H})\ \|^2 := \|\mathbf{E}\|_{0,\varepsilon}^2 + \|\mathbf{H}\|_{0,\mu}^2 \tag{24}$$

Now, the discrete energy can be rewritten as follows:

$$\mathcal{E}_h^n := \frac{1}{2}\left[\left(M^E E^n, E^n\right) + \left(M^H H^{n-\frac{1}{2}}, H^{n+\frac{1}{2}}\right)\right] = \tag{25}$$

$$= \frac{1}{2}\left[\left(M^E E^n, E^n\right) + \left(M^H H^{n-\frac{1}{2}}, H^{n-\frac{1}{2}} - \Delta t (M^H)^{-1} R^T E^n\right)\right] = \tag{26}$$

$$= \frac{1}{2}\left[\left(M^E E^n, E^n\right) + \left(M^H H^{n-\frac{1}{2}}, H^{n-\frac{1}{2}}\right) - \left(M^H H^{n-\frac{1}{2}}, \Delta t (M^H)^{-1} R^T E^n\right)\right] = \tag{27}$$

$$= \frac{1}{2}\left[\left(M^E E^n, E^n\right) + \left(M^H H^{n-\frac{1}{2}}, H^{n-\frac{1}{2}}\right) - \Delta t \left(H^{n-\frac{1}{2}}, R^T E^n\right)\right] \tag{28}$$

In which a Taylor expansion was exploited between the first and second line, and the equality $M^H(M^H)^{-1} = I$ was exploited between the third and the fourth one. It is then easy to multiply by $I = (M^E)^{-\frac{1}{2}}(M^E)^{\frac{1}{2}}$ or $I = (M^H)^{-\frac{1}{2}}(M^H)^{\frac{1}{2}}$ in the positions shown in the equation:

$$\Delta t \left[(M^H)^{-\frac{1}{2}}(M^H)^{\frac{1}{2}}\mathbf{H}^{n-\frac{1}{2}}, R^T(M^E)^{-\frac{1}{2}}(M^E)^{\frac{1}{2}}\mathbf{E}^n\right] = \tag{29}$$

$$= \Delta t \left[(\mathbf{H}^{n-\frac{1}{2}})^T(M^H)^{\frac{1}{2}}\right]\left[(M^H)^{-\frac{1}{2}}R^T(M^E)^{-\frac{1}{2}}\right]\left[(M^E)^{\frac{1}{2}}\mathbf{E}^n\right] \leq \tag{30}$$

$$\leq \Delta t \left[\|(M^H)^{-\frac{1}{2}}R^T(M^E)^{-\frac{1}{2}}\|\|\mathbf{E}\|_{0,\varepsilon}\|\mathbf{H}\|_{0,\mu}\right] \tag{31}$$

Which is due to typical matrix properties. The last passage, in particular, comes from the Cauchy-Schwarz inequality and from the compatibility property of matrix norms. Let's define the following quantities:

$$\mathbf{U} := (M^E)^{\frac{1}{2}}\mathbf{E}^n$$

$$\mathbf{V} := (M^H)^{\frac{1}{2}}\mathbf{H}^{n-\frac{1}{2}}$$

$$K := \left[(M^H)^{-\frac{1}{2}}R^T(M^E)^{-\frac{1}{2}}\right]$$

Thus, the quantity mentioned in 30 looks like:

$$\Delta t\ (K\mathbf{U}, \mathbf{V}) \leq \Delta t\|K\mathbf{U}\|\|\mathbf{V}\| \leq \Delta t\|K\|\|\mathbf{U}\|\|\mathbf{V}\| = \tag{32}$$

$$= \Delta t\|K\|\|\mathbf{E}\|_{0,\varepsilon}\|\mathbf{H}\|_{0,\mu} \tag{33}$$

Where the C.-S. inequality was taken into account, and later also the matrix norm definition. Another preparatory step is required:

$$0 \leq \left(\|\mathbf{E}\|_{0,\varepsilon} - \|\mathbf{H}\|_{0,\mu}\right)^2 = \|\mathbf{E}\|_{0,\varepsilon}^2 + \|\mathbf{H}\|_{0,\mu}^2 - 2\|\mathbf{E}\|_{0,\varepsilon}\|\mathbf{H}\|_{0,\mu} = \tag{34}$$

$$= \|\ (\mathbf{E}, \mathbf{H})\ \|^2 - 2\|\mathbf{E}\|_{0,\varepsilon}\|\mathbf{H}\|_{0,\mu} \implies \tag{35}$$

$$\|\mathbf{E}\|_{0,\varepsilon}\|\mathbf{H}\|_{0,\mu} \leq \frac{1}{2}\|\ (\mathbf{E}, \mathbf{H})\ \|^2 \tag{36}$$

Now, the only thing left to do is obtaining a majoration for discrete energy (written as in equation 28):

$$\mathcal{E}_h^n := \frac{1}{2}\left[\|\mathbf{E}\|_{0,\varepsilon}^2 + \|\mathbf{H}\|_{0,\mu}^2 - \Delta t\left(H^{n-\frac{1}{2}}, R^T E^n\right)\right] \geq \tag{37}$$

$$\geq \frac{1}{2}\left[\|\mathbf{E}\|_{0,\varepsilon}^2 + \|\mathbf{H}\|_{0,\mu}^2 - \Delta t\|K\|\|\mathbf{E}\|_{0,\varepsilon}\|\mathbf{H}\|_{0,\mu}\right] \geq \tag{38}$$

$$\geq \frac{1}{2}\left[\|\mathbf{E}\|_{0,\varepsilon}^2 + \|\mathbf{H}\|_{0,\mu}^2 - \frac{1}{2}\Delta t\|K\|\left(\|\mathbf{E}\|_{0,\varepsilon}^2 + \|\mathbf{H}\|_{0,\mu}^2\right)\right] \geq \tag{39}$$

$$\geq \frac{1}{2}\left(1 - \frac{\Delta t}{2}\|K\|\right)\|(\mathbf{E},\mathbf{H})\|^2 \tag{40}$$

Where the previous results were finally exploited. Having shown a majoration for $\mathcal{E}_h^n$, the sufficient CFL condition can be stated as follows:

Theorem 1 *For the numerical algorithm to be L^2-stable, the sum of the squared norms of the solution vectors must be limited at any time. It is clear that, for $\Delta t < \frac{2}{\|K\|}$ and for constant energy (as it is the case for homogeneous AND penalisation-free problems), this squared norm is always limited by the value of initial energy. The sufficient CFL condition is stated hereafter:*

$$\Delta t < \frac{2}{\|K\|} = \frac{2}{\left\|(M^H)^{-\frac{1}{2}}R^T(M^E)^{-\frac{1}{2}}\right\|} = \tag{41}$$

$$= \frac{2}{\sqrt{\lambda_{max}\left((M^E)^{-\frac{1}{2}}R(M^H)^{-1}R^T(M^E)^{-\frac{1}{2}}\right)}} \tag{42}$$

where the last equality follows from the definition of spectral norm:

$$\|K\| = \sqrt{\lambda_{max}\left(K^T K\right)}$$

Question 3

Q3.1

In this section, we verify that the proposed solutions in eq. 10a-b of the BE assignment are resolving the Maxwell problem in eq. 1 with the corresponding boundary conditions quoted in eq. 9. To show this, one can simply compute the derivatives of the quantities taken into account, $\mathbf{E}$ and H:

$$\mathbf{E} = \frac{m\pi}{\omega\varepsilon_0} sin(\omega t)\begin{pmatrix} cos(m\pi x)sin(m\pi y) \\ -sin(m\pi x)cos(m\pi y)\end{pmatrix} \tag{43}$$

$$H = -cos(\omega t)cos(m\pi x)cos(m\pi y) \tag{44}$$

The derivatives are taken. To synthesize the results, it is admitted that

$$S_t = sin(\omega t), \quad C_t = cos(\omega t); \tag{45}$$

$$S_x = sin(m\pi x), \quad C_x = cos(m\pi x); \tag{46}$$

$$S_y = sin(m\pi y), \quad C_y = cos(m\pi y). \tag{47}$$

$$\tag{48}$$

With these assumptions, we obtain:

$$\frac{\partial \mathbf{E}}{\partial t} = \frac{m\pi}{\varepsilon_0} C_t \begin{pmatrix} C_x S_y \\ -S_x C_y \end{pmatrix} \tag{49}$$

$$\frac{\partial H}{\partial t} = \omega S_t C_x C_y \tag{50}$$

Similarly, we proceed for the rotors of the said quantities:

$$\nabla \times \mathbf{E} = 2 S_t C_x C_y \frac{-m^2\pi^2}{\omega \varepsilon_0} \tag{51}$$

$$\nabla \times H = m\pi C_t \begin{pmatrix} C_x S_y \\ S_x C_y \end{pmatrix} \tag{52}$$

Therefore, by substituting the quantities in the Maxwell equations, and by remembering that:

$$\mathbf{J}(x, y, t) = 0 \qquad \omega = c_0 \pi m \sqrt{2} \qquad c_0 = \frac{1}{\sqrt{\varepsilon_0 \mu_0}} \tag{53}$$

we conclude that the proposed solution fulfils the problem requirements. By simply computing the solutions for $t = 0\ s$ we can also show the consistency of the solutions w.r.t. the initial condition.

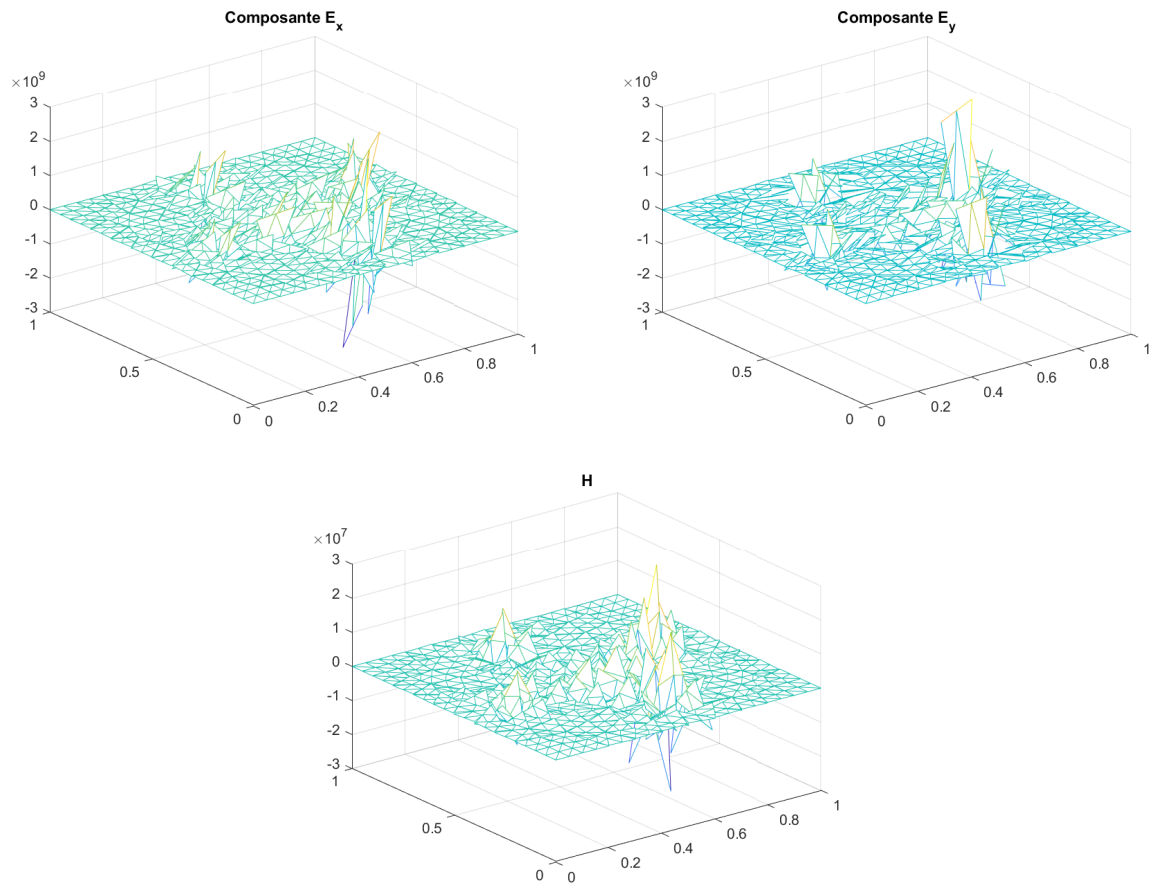

Figure 1: Fields E_x, E_y and H for the upwing scheme with the previous CFL condition. The fields explose which shows the CFL condition is not validated anymore.

Q3.3.a

The CFL condition diminishes with the polynomial order. In order to keep the stability of the algorithm, it is thus necessary to lower the time step. We get:

	1	2	3	4
CFL	0.4367	0.2421	0.1548	0.1072

Q3.3.b

The fields explodes as shown in figure 1. Indeed, the new CFL condition, for the Upwind scheme, is stronger than before, that is : it has been lowered. This means that the time step which saturated the previous CFL for the centered scheme is not anymore valid. Intuitively, we added a dissipation term to the scheme so it is now dissipative, however we do not know the sign of this term which can "play against" the stability of the scheme hence lowering the CFL.

Q3.3.c

The comparison between centered and upwind schemes is shown in figures 2. The penalisation terms smooth the solutions.

Q3.3.d

For easier reading, the L_2 norm and h_{max} have been "reduced":

- $\|L\|_{2,red}(h_i) = \frac{\|L\|_2(h_i)}{\|L\|_2(h_{min})}$
- $h_{i,red} = \frac{h_i}{h_{min}}$

Where h_{min} is the minimum h_{max} for a given k (polynomial order) and scheme (upwind or centered), for $i \in \{1, 2, 3\}$. The figure 3 shows the results, which tend to indicate the following spatial convergence order (rows for k, columns for schemes):

	centered	upwind
1	1	2
2	2	3
3	1	2

Q3.3.e

The figure 4 shows the results. Although the behaviour is clear for $k = 1$, it much less clear for others. As previously, second order polynomial is between quadratic and cubic spacial convergence. However, for the third order scheme, the convergence somewhat starts as linear and then almost goes to cubic.

The variable $\sqrt{Nb_{tri} \times N}$ is roughly the number of points per wave length when $m = 1$. In the current case, there roughly is in term of $\|E\|_2$ error, a factor 30 between first order and second order, and 5 to 10 between second order and third order. So the higher the order, the better the accuracy.

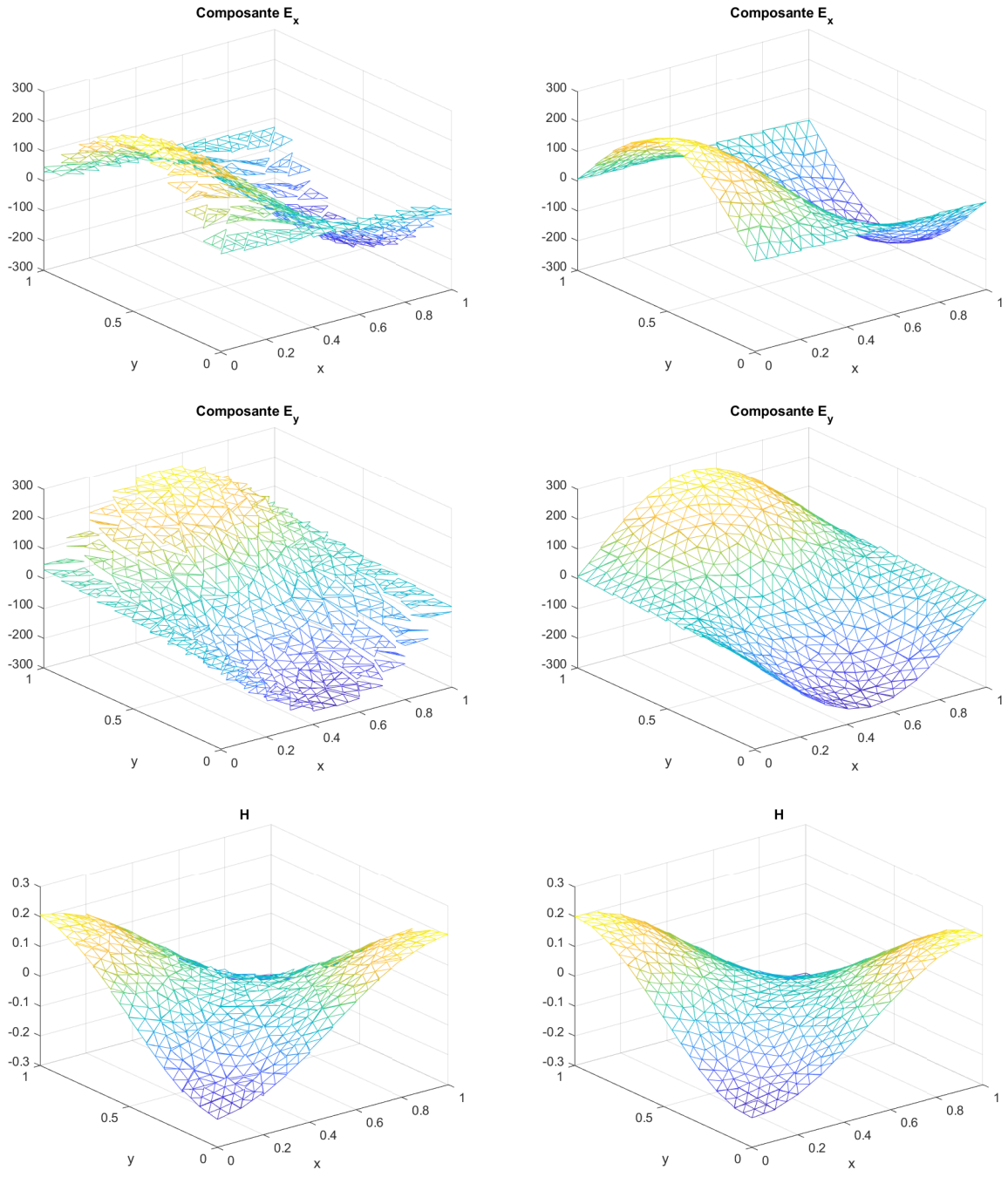

Figure 2: Fields E_x, E_y and H for the centered (left) and upwing (right) schemes with the CFL condition divided by 4. The upwind solution is better as the fields show a higher degree of smoothness.

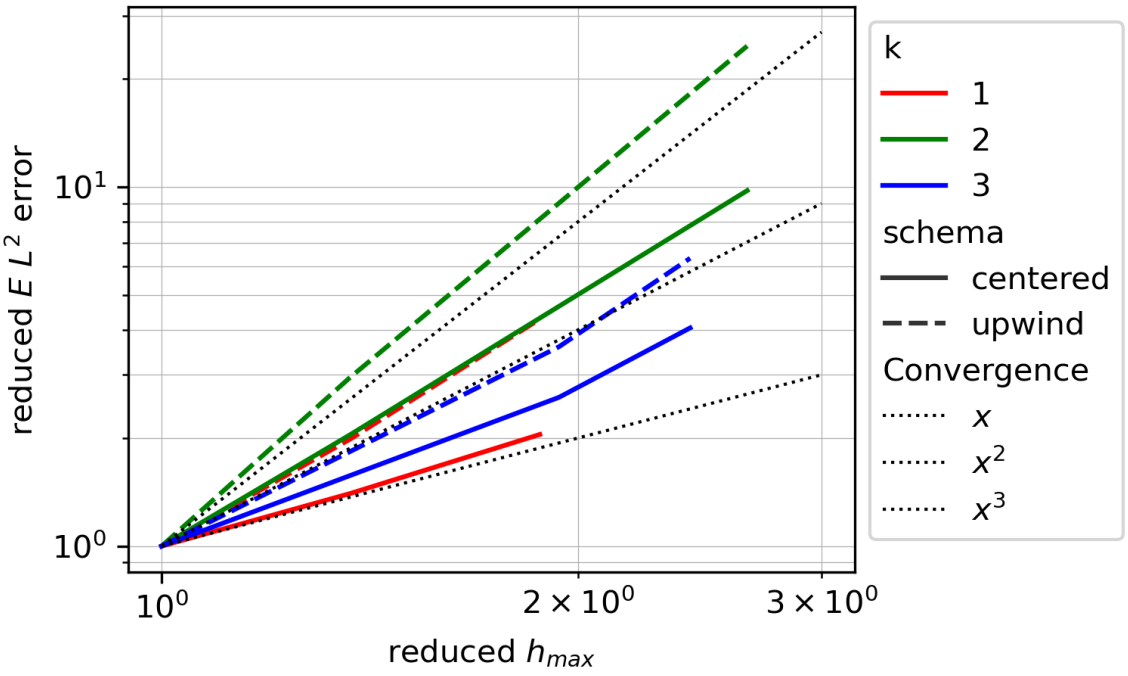

Figure 3: Log-log figure of the reduced L_2 norm as a function of the reduced h_{max} for $k \in \{1, 2, 3\}$ and centered and upwind schemes. Linear, quadratic and cubic convergence curves have been added to better see the space convergence order for the chosen configuration.

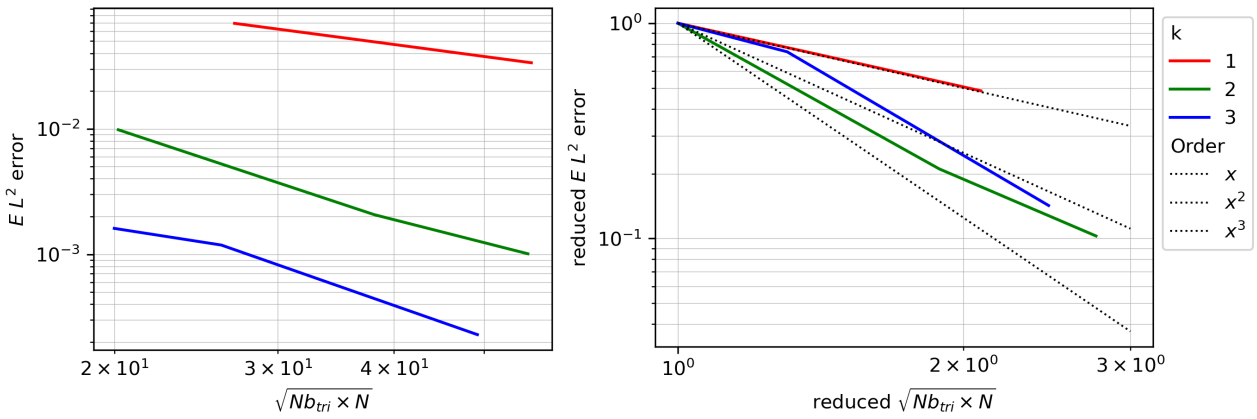

Figure 4: Log-log plot of the reduced L_2 norm as a function of $\sqrt{Nb_{tri} \times N}$ (left) or their reduced form (right) for $k \in \{1, 2, 3\}$. Linear, quadratic and cubic convergence curves have been added to better see the space convergence order for the chosen configuration.

Question 4

In this section, the interest is to show how a slightly changed formalism can cope with the integration of Maxwell's equations in presence of different boundary conditions, due to an approximation of a transparency of the domain boundaries. In addition to the differential equations and initial conditions mentioned in 6, perfectluy conductive medium is assumed on Γ_D, and Silver-Muller condition is imposed on Γ_{SM}, to simulate transparency:

$$\begin{cases} \mathbf{n} \times \mathbf{E} = 0 & on \ \ \Gamma_D \\ \mathbf{n} \times \mathbf{E} + \sqrt{\frac{\mu}{\varepsilon}} H = 0 & on \ \ \Gamma_{SM} \end{cases} \tag{54}$$

$$\tag{55}$$

where

$$\Gamma_D \cup \Gamma_{SM} = \Gamma \qquad\qquad \Gamma_D \cap \Gamma_{SM} = \emptyset \tag{56}$$

The only relevant difference in the formulation of this problem w.r.t. the one treated in Section 1 is in the boundary conditions, which are actually exploited only during the Integration By Parts. In that case, the boundary integral is affected differently w.r.t. the previous case. We start by analysing the first equation, related to electric field:

$$\frac{d}{dt} \iiint_T \varepsilon \mathbf{E}_h \cdot \mathbf{v}_h \, d\mathbf{x} - \iiint_T H_h \cdot (\nabla \times \mathbf{v}_h) \, d\mathbf{x} + \oiint_{\partial T \setminus \Gamma} (\{\{H_h\}\} \times \mathbf{n}) \cdot \mathbf{v}_{h|T} \, d\gamma + \tag{57}$$

$$+ \oiint_{\partial T \cap \Gamma} (H_h \times \mathbf{n}) \cdot \mathbf{v}_{h|T} \, d\gamma + \alpha_E \oiint_{\partial T \setminus \Gamma} \left([\![\mathbf{n}_h \times \mathbf{E}_h]\!] \right) \cdot \left(\mathbf{n}_h \times \mathbf{v}_{h|T} \right) \, d\gamma = \iiint_T \mathbf{J} \cdot \mathbf{v}_h \, d\mathbf{x} \tag{58}$$

Which, after a second IBP, is reduced to:

$$\frac{d}{dt} \iiint_T \varepsilon \mathbf{E}_h \cdot \mathbf{v}_h \, d\mathbf{x} - \iiint_T (\nabla \times H_h) \cdot \mathbf{v}_h \, d\mathbf{x} + \frac{1}{2} \oiint_{\partial T \setminus \Gamma} \left(\mathbf{n} \times [\![H_h]\!] \right) \cdot \mathbf{v}_{h|T} \, d\gamma + \tag{59}$$

$$+ \alpha_E \oiint_{\partial T \setminus \Gamma} \left([\![\mathbf{n}_h \times \mathbf{E}_h]\!] \right) \cdot \left(\mathbf{n}_h \times \mathbf{v}_{h|T} \right) \, d\gamma = \iiint_T \mathbf{J} \cdot \mathbf{v}_h \, d\mathbf{x} \tag{60}$$

This equation, actually, doesn't need to change when the problem changes, because the boundary condition is not involved, as it was formulated in terms of $\mathbf{E}$, whereas the integrals here involve only H. The major changes will need to be applied to the second equation. We analyse it starting from the very beginning:

$$\mu \frac{\partial H}{\partial t} + \nabla \times \mathbf{E} = 0 \implies$$

$$\frac{d}{dt} \iiint_T \mu H w_h \, d\mathbf{x} + \iiint_T (\nabla \times \mathbf{E}) \cdot w_h \, d\mathbf{x} = 0$$

Now, considering the following formula for the integration by parts:

$$\iiint_T (\nabla \times \mathbf{E}) \cdot w_h \, d\mathbf{x} = \iiint_T (\nabla \times w_h) \cdot \mathbf{E} \, d\mathbf{x} - \oiint_{\partial T} (\mathbf{E} \times \mathbf{n}) \cdot w_h \, d\gamma$$

We eventually substitute in the former equation, to obtain:

$$\frac{d}{dt} \iiint_T \mu H w_h \, d\mathbf{x} + \iiint_T (\nabla \times w_h) \cdot \mathbf{E} \, d\mathbf{x} - \oiint_{\partial T} (\mathbf{E} \times \mathbf{n}) \cdot w_h \, d\gamma = 0$$

In which the penalisation term was neglected, as it is not supposed to change in any way. The change is contained in the boundary term, which will be split on the pieces of the domain surface, as this enables the application of boundary-specific conditions:

$$\begin{aligned}\oiint_{\partial T} (\mathbf{E}\times\mathbf{n})\cdot w_h\,d\gamma = \\ \oiint_{\partial T\cap\Gamma_D} (\mathbf{E}\times\mathbf{n})\cdot w_h\,d\gamma + \\ + \oiint_{\partial T\cap\Gamma_{SM}} (\mathbf{E}\times\mathbf{n})\cdot w_h\,d\gamma + \\ + \oiint_{\partial T\setminus\Gamma} (\mathbf{E}\times\mathbf{n})\cdot w_h\,d\gamma\end{aligned}$$

Therefore:

- The first term in RHS is clearly null, as follows from the perfect conductivity condition on that part of the boundary.
- The second term in RHS can be elaborated further:

$$\oiint_{\partial T\cap\Gamma_{SM}} (\mathbf{E}\times\mathbf{n})\cdot w_h\,d\gamma = \oiint_{\partial T\cap\Gamma_{SM}} \sqrt{\frac{\mu}{\varepsilon}} H_h w_h\,d\gamma$$

- The third term is elaborated as for the initial Maxwell's problem, where we ended up with:

$$\begin{aligned}\oiint_{\partial T\setminus\Gamma} (\mathbf{E}\times\mathbf{n})\cdot w_h\,d\gamma \\ = \oiint_{\partial T\setminus\Gamma} \{\{\mathbf{E}_h\}\}\cdot\left(\mathbf{n}\times w_{h|T}\right)\,d\gamma\end{aligned}$$

At the end of such manipulations, the second equation of the Maxwell's problem turns out to be:

$$\begin{aligned}\frac{d}{dt}\iiint_T \mu H_h w_h\,d\mathbf{x} + \iiint_T \mathbf{E}_h\cdot(\nabla\times w_h)\,d\mathbf{x} + \alpha_H \oiint_{\partial T\setminus\Gamma} \left(\left[\!\left[\mathbf{n}_h\times H_h\right]\!\right]\right)\cdot\left(\mathbf{n}_h\times w_{h|T}\right)\,d\gamma + \\ - \oiint_{\partial T\setminus\Gamma} \{\{\mathbf{E}_h\}\}\cdot\left(\mathbf{n}\times w_{h|T}\right)\,d\gamma - \oiint_{\partial T\cap\Gamma_{SM}} \sqrt{\frac{\mu}{\varepsilon}} H_h w_h\,d\gamma = 0\end{aligned}$$

Which is what was meant to be shown.

Question 5

The evolution of E_y displays the circular wave expanding from the source outward, with a variation in value on the wave front. Two such waves (with opposite signs though) are successively produced. The figure 5 shows two frames of the simulation (the 340th iteration to the left and the last iteration to the right) for E_y. On the left one, one can observe the two waves : the first one is reaching the bounds of the system, while the first one is still somewhat close to the source. In agreement with the Silver-Müller condition, the wave is not reflected in any way and the DG solver is behaving correctly.

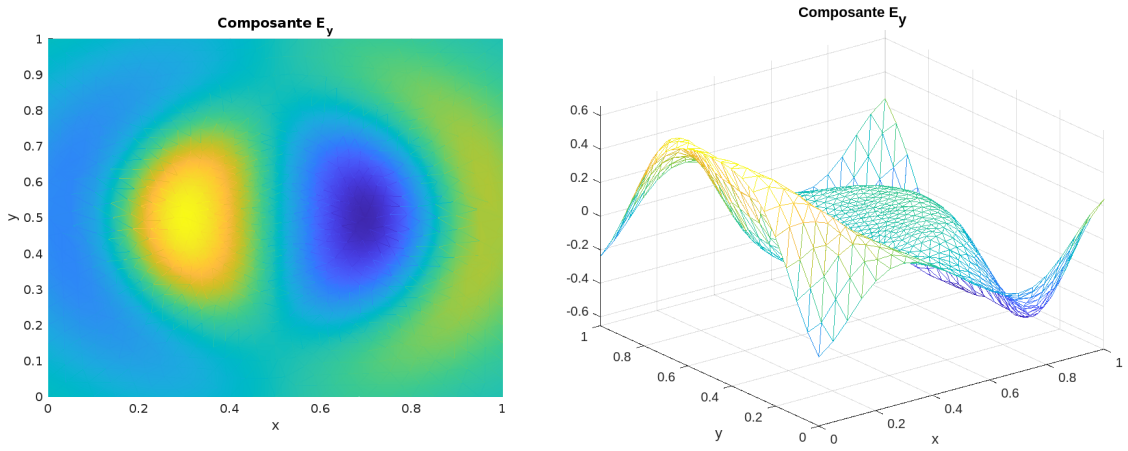

Figure 5: E_y is shown at two time steps - the 340^{th} one to the left, and the last one to the right. The wave value is varying on its front with the upmost and nethermost having 0 as value, thus yielding the impression that two waves are moving : one at x decreasing, the other at x increasing.

Question 6

The space is composed of two dielectrics. A source is located in the lower region which is characterised by a relative permittivity of 1 while the upmost region is 4. The surface between the two dielectrics is not charged, thus one can expect from the vectorized transition equation the equality (see equation below) of both regions electrical fields. One can even computes the the ratio of the incident wave which is transmitted and refracted.

$$\vec{E_2} - \vec{E_2} = \frac{\sigma}{\epsilon_0}\vec{n_{1,2}} \tag{61}$$

$$r = \frac{n_1 - n_2}{n_1 + n_2} \tag{62}$$

$$t = \frac{2n_1}{n_1 + n_2} \tag{63}$$

With $n^2 = \epsilon_r$. With previously stated value, this yields : $r = -\frac{1}{3}$ and $t = \frac{2}{3}$. It is hard to check weather the ratios are verified or not in practice, however the continuity is easier (on the tangential component, that is E_x).

In practice, we observe quite clearly with the film that when the first wave reaches the boundary between the two regions, a portion of it is reflected while the rest is transmitted. The figure 6 shows the last iteration of the simulation and shows quite clearly that while the x electric field component seems to verify continuity at the boundary, the y component clearly does not. However, no condition on continuity is imposed and it can thus be a viable solution. The the DG scheme seems to work too in this case.

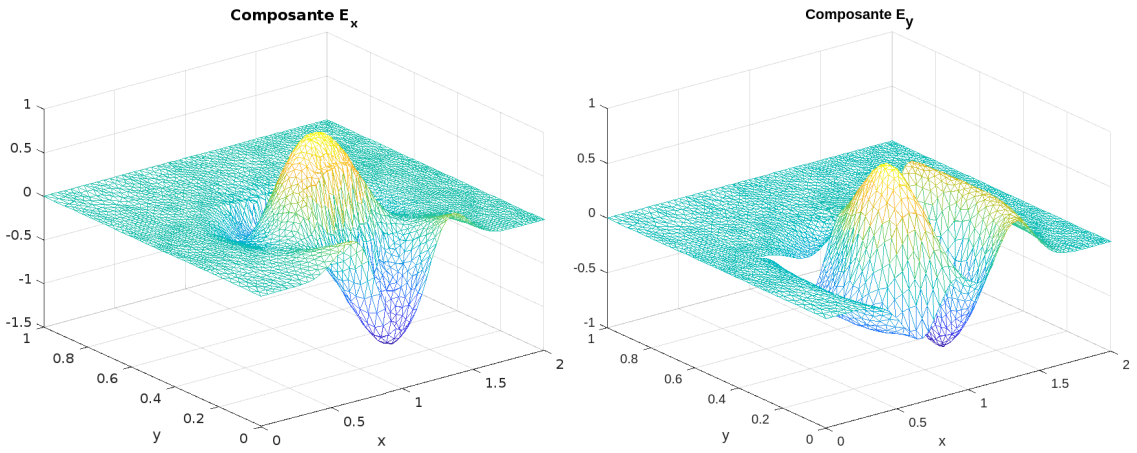

Figure 6: Electric field components E_x (left) and E_y (right) at the end of the simulation.

Question 7

Continous Model

In this section a new problem is proposed. Here are its main features:

- The unit disk $\mathcal{D}((2,1),1)$, assumed as a perfectly conductive medium, diffracts the incoming radiation generated by a source s of known coordinates and width.
- The radiation propagates in free space away from the disk, fact which is simulated by adding a Silver-Muller transparency condition on a "virtual" external boundary of the domain.
- The domain model Ω is a box-like domain (an empty cavity) with a hole corresponding to the disk (which is full, instead).
- Boundary Γ of the domain is so defined:

$$\Gamma = \Gamma_D \cup \Gamma_{SM}$$

  where Γ_D is the unit circle and witnesses a radially-pointing Electrical Field.Γ_{SM}, instead, is the Silver-Muller domain, corresponding with the outer boundaries of the box.

- The source has a centre in $(x_s, y_s) = (0.5, 1)$ and a radius $r_s = 0.25$

The model is nearly the same as in Question 4, apart from a different shape of the domain.

$$\begin{cases} \varepsilon \frac{\partial \mathbf{E}}{\partial t} - \nabla \times H = \mathbf{J}_s(\mathbf{x}, t) \quad in \ \ \Omega \\ \mu \frac{\partial H}{\partial t} + \nabla \times \mathbf{E} = 0 \quad in \ \ \Omega \\ \mathbf{n} \times \mathbf{E} = 0 \quad on \ \Gamma_D \\ \mathbf{n} \times \mathbf{E} + \sqrt{\frac{\mu}{\varepsilon}} H = 0 \quad on \ \Gamma_{SM} \\ \mathbf{E}(\mathbf{x}, 0) = \mathbf{E}_0 \quad in \ \ \Omega \\ H(\mathbf{x}, 0) = H_0 \quad in \ \ \Omega \end{cases} \tag{64}$$

These equations will ensure that the disk diffracts incoming radiations, which in turn will "flow" away from it.

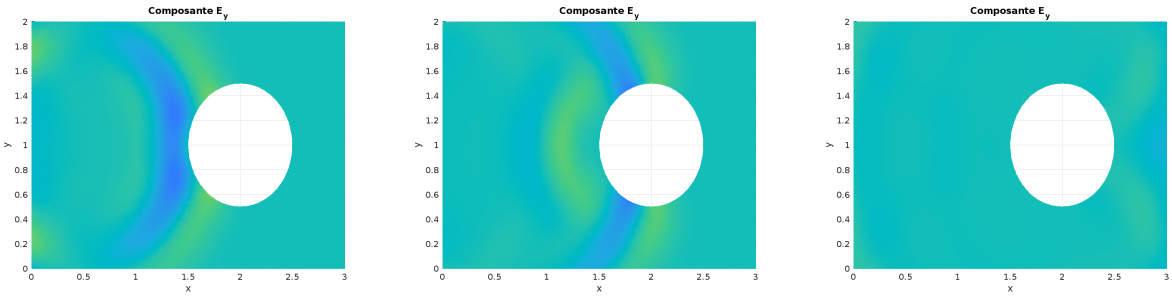

Figure 7: Electric field components E_y at three different iterations. On the left picture, the extinction of the field is clearly visible on the left side of the disk. On the middle picture, one can see the waves reflection and also, at the top and bottom points of the disk, the electric field that are not forced to 0 anymore. However, it is hard to see the recombination of the waves in the right picture: as the waves spread, its energy is spread on a bigger front and the amplitude diminishes yielding in our case very poor contrast compared to the first pictures. The numerical viscosity also decreases the energy in the system and could cause similar observations.

Discontinuous Galerkin Model

Following from the previous model, we end up with a discretised variational model alike to that mentioned in Question 4.

$$\mathbf{I}: \quad \frac{d}{dt}\iiint_T \varepsilon \mathbf{E}_h \cdot \mathbf{v}_h \, d\mathbf{x} - \iiint_T (\nabla \times H_h) \cdot \mathbf{v}_h \, d\mathbf{x} + \frac{1}{2}\oiint_{\partial T \setminus \Gamma} (\mathbf{n} \times [\![H_h]\!]) \cdot \mathbf{v}_{h|T} \, d\gamma + \\ + \alpha_E \oiint_{\partial T \setminus \Gamma} ([\![\mathbf{n}_h \times \mathbf{E}_h]\!]) \cdot (\mathbf{n}_h \times \mathbf{v}_{h|T}) \, d\gamma = \iiint_T \mathbf{J}_s \cdot \mathbf{v}_h \, d\mathbf{x}$$

$$\mathbf{II}: \quad \frac{d}{dt}\iiint_T \mu H_h w_h \, d\mathbf{x} + \iiint_T \mathbf{E}_h \cdot (\nabla \times w_h) \, d\mathbf{x} + \alpha_H \oiint_{\partial T \setminus \Gamma} ([\![\mathbf{n}_h \times H_h]\!]) \cdot (\mathbf{n}_h \times w_{h|T}) \, d\gamma + \\ - \oiint_{\partial T \setminus \Gamma} \{\{\mathbf{E}_h\}\} \cdot (\mathbf{n} \times w_{h|T}) \, d\gamma - \oiint_{\partial T \cap \Gamma_{SM}} \sqrt{\frac{\mu}{\varepsilon}} H_h w_h \, d\gamma = 0$$

Numerical Solution and Visualisation

The simulation shows the waves reflecting on the metal disk and leaving the system as expected from the Silver-Müller condition. The two waves seem to recombine after the obstacle, however the figure is not very clear, and the mesh stops at $x = 3$ which prevents a full observation. We also expect that at the left side of the disk, the E_y value should be close to 0 and even 0 at the farthest point (x min) because of the continuity of the tangential field. Close to the utmost and nethermost points of the disk, the y-component of the electric field should not go to 0 anymore as no continuity condition applies for the normal-to-the-disk electric field component, in this case E_y. Thus, from a quantitative perspective, nothing seems amiss and the DG scheme seems to provide a physically feasible solution. Figure 7 shows some iterations for E_y.

Question 8: Final Comments

In this report, we observed that the DG method, contrary to the common Finite Elements Method, for instance, allows to change the mesh and the physics without too much trouble. It is also possible to increase the scheme order (we went up to third order) which can be hard for, say, the finite volume methods.

In addition to these statements comparing methods, specific remarks can be made:

- The time resolution, that is Δt step, is very important for the continuity of the solution as was shown in Question 3) when comparing the centered and upwind schemes. In relation to that, rough numerical solutions are characterised by a low level of continuity.
- For the upwind scheme (or generally speaking the penalised ones), it is important to notice the effect of dissipation which decreases energy with a numerical viscosity and in turn smoothens the solution. Nevertheless, some of the slightest features of the solution are lost.
- Increasing the schema order yields more accurate results, all things being equal, as shown in Question 3.3.e for the centered schema.
- Although, increasing the order yields more accurate results, the order of convergence may differ from one polynomial order to the next. Judging from Q3.3.d, we may think that it is better to select even polynomial order to increase order of convergence. A thorough analysis is nonetheless required to verify this statement rigorously.
- The DG schema can handle a variety of meshes and even heterogeneous space with regions of different physics quantities as illustrated in Question 6.